© 2018. Published by The Company of Biologists Ltd | Development (2018) 145, dev159624. doi:10.1242/dev.159624

RESEARCH ARTICLE

Conserved functional control, but distinct regulation, of cell proliferation in rice and *Arabidopsis* leaves revealed by comparative analysis of *GRF-INTERACTING FACTOR 1* orthologs

Satomi Shimano[1], Ken-ichiro Hibara[1], Tomoyuki Furuya[2], Shin-ichi Arimura[1], Hirokazu Tsukaya[2,3] and Jun-Ichi Itoh[1,*]

ABSTRACT

Regulation of cell proliferation is crucial for establishing the shape of plant leaves. We have identified *MAKIBA3* (*MKB3*), a loss-of-function mutant of which exhibits a narrowed- and rolled-leaf phenotype in rice. *MKB3* was found to be an ortholog of *Arabidopsis ANGUSTIFOLIA3* (*AN3*), which positively regulates cell proliferation. The reduced leaf size of *mkb3* plants with enlarged cells and the increased size of *MKB3*-overexpressing leaves with normal-sized cells indicate that *MKB3* is a positive regulator of leaf proliferation and that *mkb3* mutation triggers a compensation syndrome, as does *Arabidopsis an3*. Expression analysis revealed that *MKB3* is predominantly expressed on the epidermis of leaf primordia, which is different from the location of *AN3*. A protein movement assay demonstrated that MKB3 moves from an *MKB3*-expressing domain to a non-expressing domain, which is required for normal leaf development. Our results suggest that rice *MKB3* and *Arabidopsis AN3* have conserved functions and effects on leaf development. However, the expression pattern of *MKB3* and direction of protein movement are different between rice and *Arabidopsis*, which might reflect differences in leaf primordia development in these two species.

KEY WORDS: *MKB3*, *GIF1*, *AN3*, Rice, Leaf development, Protein movement

INTRODUCTION

Leaves are major above-ground parts in most plant species. Leaf size and shape is species specific, but leaf primordium development begins as a lateral protrusion of the shoot apical meristem (SAM) in all plant species. The variation in leaf size and shape is determined by several developmental processes driven by common and diverged genetic programs after leaf initiation. Genetic variation and conservation of these programs during leaf development is a major topic in plant developmental biology (Tsukaya, 2014, 2017).

Regulation of cell proliferation is an important determinant of leaf size and shape (Ichihashi and Tsukaya, 2015; Tsukaya, 2017). Thus, many genes associated with leaf cell proliferation have been analyzed (Gonzalez et al., 2012; Nelissen et al., 2016). Members of the *TEOSINTE-BRANCHED1*/*CYCLOIDEA*/*PCF* (*TCP*) and *NGATHA* (*NGA*) gene families, which encode plant-specific transcriptional factors, are involved in several aspects of leaf development by repressing cell proliferation in the marginal meristems of leaves of the snap dragon, *Arabidopsis*, tomato, creeping bentgrass and rice (Ori et al., 2007; Efroni et al., 2008; Hervé et al., 2009; Kieffer et al., 2011; Yang et al., 2013; Zhou et al., 2013; Alvarez et al., 2016). *KLUH* (*KLU*) and *PLASTOCHRON1* (*PLA1*) are other type of regulators of cell proliferation during leaf development in *Arabidopsis* and rice, respectively (Miyoshi et al., 2004; Anastasiou et al., 2007; Mimura and Itoh, 2014). *KLU*/*PLA1* encodes a member of the cytochrome P450 monooxygenase subgroup, *CYP78A*, although its substrate is unknown. Because loss-of-function mutants of *KLU* and *PLA1* exhibited smaller leaves with fewer cells, *KLU*/*PLA1* was proposed to be involved in production of an unknown signaling molecule that positively regulates cell proliferation in leaves (Anastasiou et al., 2007). Overexpression of *KLU*, *PLA1* and *ZmPLA1*, which are maize *PLA1* orthologs, resulted in larger leaves and reproductive organs, indicating that *KLU*/*PLA1* positively regulates cell proliferation (Hibara et al., 2016; Sun et al., 2017).

GROWTH-REGULATING FACTOR (GRF) genes are plant-specific transcriptional regulators that play important roles in the regulation of cell proliferation (Kim and Tsukaya, 2015). The *Arabidopsis* genome harbors nine GRF genes, most of which are expressed in organs and tissues with high growth activity, and positively regulate cell proliferation (Kim et al., 2003; Horiguchi et al., 2005; Kim and Lee, 2006). In addition, seven out of the nine GRF genes are targeted by the microRNA *miR396*; thus, the site of GRF action is dependent on the *miR396* accumulation pattern (Jones-Rhoades and Bartel, 2004; Liu et al., 2009; Rodriguez et al., 2010; Wang et al., 2011). In monocot species such as rice and maize, most GRF genes positively regulate cell proliferation during leaf development by a mechanism similar to that in *Arabidopsis* (van der Knaap et al., 2000; Choi et al., 2004; Li et al., 2010; Nelissen et al., 2015), although maize *ZmGRF10* reportedly negatively regulates cell proliferation (Wu et al., 2014).

GRF-INTERACTING FACTOR (GIF) genes also control cell proliferation during leaf development (Kim and Tsukaya, 2015). GIF was first identified as a protein partner that physically interacts with GRFs. GIFs function as transcriptional co-activators for GRFs and other transcription factors by forming complexes with SWI2/SNF2 chromatin remodeling-related proteins (Vercruyssen et al., 2014). Among the three GIF genes in the *Arabidopsis* genome, *GIF1*, also

[1]Graduate School of Agricultural and Life Sciences, The University of Tokyo, Tokyo 113-8657, Japan. [2]Department of Biological Sciences, Faculty of Science, The University of Tokyo, 7-3-1 Hongo, Bunkyo-ku, Tokyo 113-0033, Japan. [3]Bio-Next Project, Okazaki Institute for Integrative Bioscience, National Institutes of Natural Sciences, Yamate Building #3, 5-1, Higashiyama, Myodaiji, Okazaki, Aichi 444-8787, Japan.

*Author for correspondence (ajunito@mail.ecc.u-tokyo.ac.jp)

J.-I.I., 0000-0001-8952-2697

Received 21 September 2017; Accepted 13 March 2018

Development (2018) 145, dev159624. doi:10.1242/dev.159624

known as *ANGSTIFOLIA3* (*AN3*), positively regulates cell division in young leaf primordia (Kim and Kende, 2004; Horiguchi et al., 2005). Importantly, in *Arabidopsis* leaf primordia, *AN3/AtGIF1* mRNA is detected only in mesophyll cells of the basal part of leaf primordia (Kawade et al., 2013) and AN3/AtGIF1 protein moves between cells between epidermis and parenchymatous cells (Kawade et al., 2013), which is required for proper leaf organogenesis. Recently, it has been shown that the AN3/AtGIF1 protein is required to move among cells lying along the longitudinal axes of leaf primordia to ensure appropriate positioning of the leaf plate meristem (Kawade et al., 2017). Although *GIF1*, *GIF2* and *GIF3* redundantly regulate various aspects of plant development (Kim and Kende, 2004; Lee et al., 2009, 2014), a single loss-of-function mutation in *AN3*/*GIF1* resulted in smaller and narrower leaves with reduced cell proliferation (Horiguchi et al., 2005; Vercruyssen et al., 2014). In grass species, the functions of *GIF1* orthologs are largely conserved, as are the proteins with which these factors interact (Nelissen et al., 2015). OsGIFs physically interact with OsGRF4/GLW2, OsGRF6 and OsGRF10, and activate their transcription (Liu et al., 2014; Li et al., 2016).

Compensation is a phenomenon closely related to cell proliferation in leaves (Tsukaya, 2002; Hisanaga et al., 2015). It is post-mitotic cell expansion in leaves that occurs when the cell number is decreased by mutations or overexpression of cell proliferation-related genes. The *an3* mutant shows typical compensation syndrome, exhibiting smaller leaves with a reduced number of enlarged cells. Cell enlargement is not a direct effect of loss of *AN3* function, because overexpression of *AN3* does not affect cell size (Kim and Kende, 2004; Horiguchi et al., 2005; Lee et al., 2009). Similarly, overexpression of a cyclin-dependent kinase inhibitor gene, *KRP2*, in *Arabidopsis* resulted in suppressed cell proliferation and enlarged cells in leaves (Ferjani et al., 2013a,b). In addition, it has been revealed, using kinetic and genetic analysis of cell size enlargement, that the mechanisms that trigger compensation in *an3* mutant and *KRP2*-overexpressing plants are different (Kawade et al., 2010; Ferjani et al., 2013b; Hisanaga et al., 2015). In rice, overexpression of a cyclin-dependent kinase inhibitor homolog, *OsKRP1*, induced cell enlargement by compensating for the reduced cell number. Thus, compensation occurs in diverse plant species (Barrôco et al., 2006; Horiguchi and Tsukaya, 2011).

Several pathways and mechanisms involved in leaf development are conserved among plant species. However, knowledge of how common genetic factors exert their functions in different developmental backgrounds is limited. In this study, we evaluated the phenotypic effects of loss of function and overexpression of rice *MAKIBA3* (*MKB3*), an ortholog of *Arabidopsis AN3*. Expression analysis and use of a protein movement assay revealed the functional conservation, but divergent regulation, of orthologous genes in the two species.

RESULTS

Phenotype of the *mkb3* mutant during vegetative development

mkb3 was identified as a recessive mutant that showed an abnormal leaf morphology. As *mkb3* roots exhibited no obvious abnormality (Fig. S1), we investigated the gross leaf phenotype of *mkb3*. Because *mkb3* showed shortened and narrowed leaves (Fig. 1A), we measured several parameters in the fifth leaf of *mkb3* and the wild

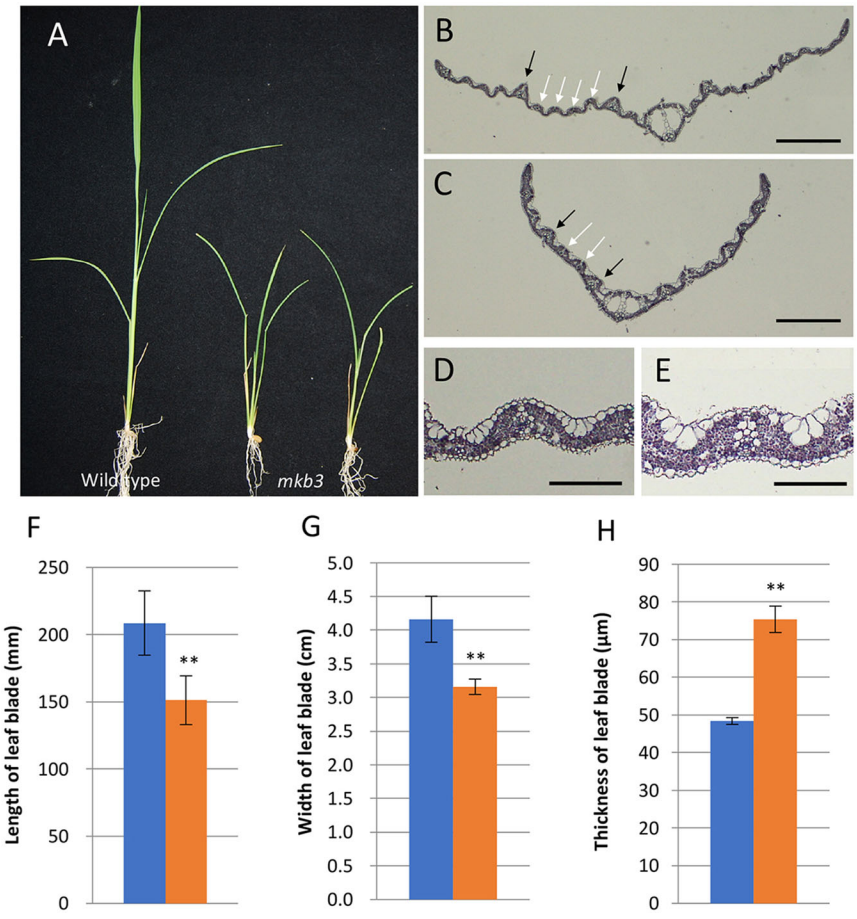

Fig. 1. Leaf phenotypes of *mkb3*. (A) Seedlings of wild type (left) and *mkb3* mutant (center and right) 21 days after germination. (B,C) Cross-section of the 5th leaf blade in wild type (B) and *mkb3* (C). Black and white arrows indicate the positions of large and small vascular bundles, respectively. (D,E) Higher-magnification views of the cross-sections of leaf blades from wild type (D) and *mkb3* (E). (F) Length of fifth leaf blade. (G) Width of fifth leaf blade. (H) Thickness of fifth leaf blade. Scale bars: 500 µm in B,C; 100 µm in D,E. *n*=5 in F-H. Data are mean±s.e.m. and are significantly different from wild type where indicated, as assessed by Student's *t*-test (***P*<0.01).

Development (2018) 145, dev159624. doi:10.1242/dev.159624

type. The length and width of the leaf blade were reduced by 72% and 75% compared with the wild type, respectively (Fig. 1F,G). In contrast, cross-sections revealed that the fifth leaf of the *mkb3* leaf blade is rolled adaxially and was 156% thicker than that of the wild type (Fig. 1B,C,H).

To understand how the reduction in leaf size is related to the cell size of *mkb3* leaves, we evaluated the size of epidermal cells along the proximal-distal, medial-lateral and adaxial-abaxial axes of the leaf (Table 1). The length of adaxial epidermal cells of the leaf sheath along the proximal-distal axis in *mkb3* plants was significantly greater than in the wild type. The width of epidermal cells of the abaxial leaf blade along the medial-lateral axis in the *mkb3* mutant was slightly larger, and the thickness of bulliform cells, which are specialized epidermal cells on the adaxial surface of the leaf blade, was significantly greater in *mkb3* plants than in the wild type (Fig. 1D,E and Table 1). Accordingly, cells were generally enlarged along all axes of the leaf, despite the reduced leaf size along the proximal-distal and medial-lateral axes. Therefore, the number of cells along the proximal-distal and medial-lateral axes in leaves of *mkb3* plants were calculated to be lower than that in wild type, but those along the adaxial-abaxial axis are unaffected.

Cell enlargement is often accompanied by increased nuclear ploidy. In some plant species, endoreduplication, which is DNA replication without mitosis, leads to increased leaf ploidy often correlated with epidermal cell size (Katagiri et al., 2016). Thus, the ploidy level of wild-type and *mkb3* leaves was analyzed, although endoreduplication does not normally occur in rice leaves. The ploidy level of *mkb3* leaves was normal, i.e. only the 2C peak was observed in both wild-type and *mkb3* leaves (Fig. S2). Therefore, cell enlargement in the *mkb3* mutant is not caused by endoreduplication.

We also investigated the vascular differentiation of wild-type and *mkb3* plants using the fifth leaf blade (Table 1). Although the morphology of the vascular bundles was not changed (Fig. 1D,E), the number of small vascular bundles in the *mkb3* mutant was significantly reduced. However, the intervals between vascular bundles were slightly increased (Fig. 1B,C). This indicates that the *mkb3* mutation leads to a reduced number of vascular bundles, reflecting the reduced leaf width (Russell and Evert, 1985; Dannenhoffer et al., 1990), but the intervals between the vascular bundles were not influenced by the reduction in the leaf size.

Phenotype of the *mkb3* mutant in reproductive development

mkb3 plants produced a panicle significantly reduced in length (Fig. 2A,B). In the wild type, the internode length decreases gradually from top to bottom. The *mkb3* mutant also showed this tendency, but the top two internodes were greatly reduced in length (Fig. 2A,B). The length of the primary rachis branches was also reduced, but their number was not affected, indicating that *MKB3* is involved in the elongation of internodes and rachis branches during panicle development (Fig. 2C-E).

mkb3 spikelets also exhibited morphological abnormalities. The shape of the lemma and the palea was distorted, and the width of the palea was significantly reduced (Fig. 2F,G). Although the number and shape of floral organs (lodicule, stamen and pistil) were not affected (Fig. 2H,I), differentiation of pollen in *mkb3* anthers was incomplete (Fig. S3). In addition, abnormalities in integument elongation and ovule formation were observed in some *mkb3* pistils (Fig. 2J,K). Therefore, *MKB3* is also required for the differentiation of some floral tissues. These abnormalities may be the cause of the sterility of the *mkb3* mutant.

Table 1. Effect of *mkb3* on cell size and the inner structures of leaves

	Wild type	*mkb3*
Length of epidermal cells (μm)*	124.1±15.2	150.8±8.9**
Width of epidermal cells (μm)‡	10.8±0.4	12.5±1.6
Thickness of bulliform cells (μm)‡	26.2±1.2	34.5±4.5*
Number of large vascular bundles‡	6.4±0.5	6.8±0.4
Number of small vascular bundles‡	19.4±0.9	10.6±1.3**
Interval between vascular bundles (μm)‡	166.3±17.4	173.9±17.5

*The values were measured using adaxial epidermal cells of the fifth leaf sheath.

‡The values were measured using the fifth leaf blade.

n=25 for cell size, *n*=5 for vascular traits. Data marked with single or double asterisks significantly differ from those of the wild type, as assessed using Student's *t*-test to compare epidermal cell sizes and vascular intervals, and the Mann-Whitney test to compare vascular numbers. *P<0.05 and **P<0.01.

Identification of *MKB3*

We next identified *MKB3* by a map-based cloning strategy. Rough and fine mapping using *mkb3* homozygous plants derived from an F_2 population crossed between *mkb3* heterozygotes and cv. Kasalath (wild type) predicted that the mutation was located between two markers on chromosome 3 (Fig. 3A). Among the predicted genes in two BAC contigs, we found a base substitution from G to A at the 3′ splicing site of the third intron of *Os03g0733600* (Fig. 3A). *Os03g0733600* was predicted to be an SSXT family protein with homology to the human transcription co-activator synovial sarcoma translocation protein.

To confirm that this mutation in *Os03g0733600* was responsible for the phenotype of *mkb3*, a 8251 bp fragment of *Os03g0733600*, including the 3308 bp putative promoter and 1898 bp terminator regions, was introduced into *mkb3* calli. The regenerated plants harboring the *Os03g0733600* fragment showed a normal phenotype, whereas plants regenerated with empty vector had narrow, rolled leaf blades, identical to the *mkb3* mutant (Fig. 3C,D). These data confirmed that *Os03g0733600* is *MKB3*.

Phylogenetic analysis in several plant species revealed that *MKB3* is an ortholog of *AN3*/*GIF1*, which functions as a transcriptional co-activator and positively regulates cell proliferation by interacting with *GRF* transcriptional regulators in *Arabidopsis* (Fig. 3E and Fig. S4), although the extent of amino acid identity and similarity between MKB3 and AN3 were not high: 50% and 57%, respectively. MKB3 protein has a conserved SNH domain, which is required for the interaction with GRF, at the N terminus (Fig. 3B) (Kim and Tsukaya, 2015). Accordingly, MKB3 is predicted to regulate cell proliferation by interacting with GRFs. Indeed, direct interaction between OsGIF1 (a synonym of MKB3) and GRFs has been reported (Duan et al., 2015). The *mkb3* mutation generates a premature stop codon between the SNH domain of the N terminus and the glutamine- and glycine-rich domain of the C terminus of the MKB3 protein, which may indicate that the C termini of *GIF1* homologs play important roles (Fig. 3A and Fig. S4).

To explore whether *MKB3* was functionally equivalent to *Arabidopsis* AN3, we performed an interspecific complementation test. Introduction of *MKB3* cDNA fused with *GFP* under the control of the *AN3* promoter into the *an3-4* strain almost rescued the leaf phenotypes (Fig. 3F,G,J and Fig. S5), as did the introduction of *AN3-GFP* (Fig. 3F-H and Fig. S5), indicating that *AN3* can be substituted by *MKB3* and that the protein functions are conserved between rice and *Arabidopsis*.

Expression of *MKB3*

To assess the *MKB3* expression pattern during the plant life cycle, we searched the rice gene expression database RiceXPro

Development (2018) 145, dev159624. doi:10.1242/dev.159624

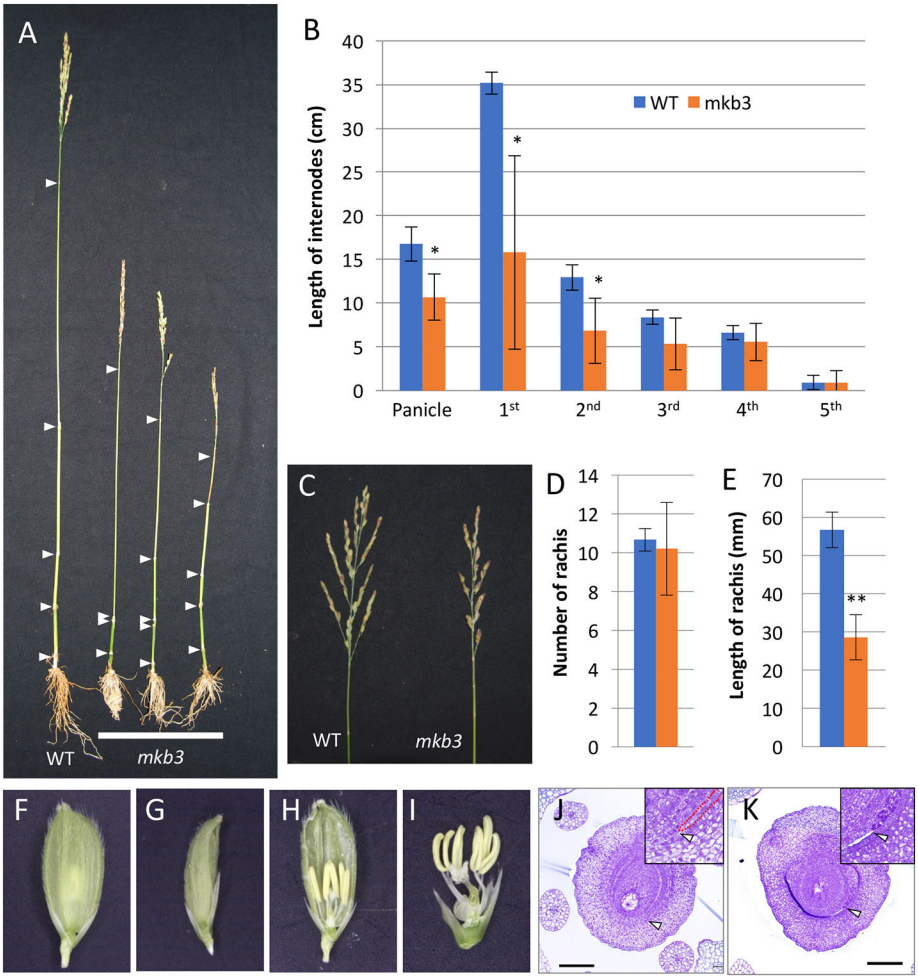

Fig. 2. Phenotypes of *mkb3* in reproductive development. (A) Elongation of internodes of mature plants in wild type (left) and *mkb3* (right). White arrowheads indicate the positions of the nodes. (B) Lengths of the internodes. (C) Panicles of wild type (left) and *mkb3* (right). (D) Numbers of primary rachis branches. (E) Lengths of primary rachis branches. (F,G) Spikelets of wild type (F) and *mkb3* (G). (H,I) Floral organs of wild type (H) and *mkb3* (I). Palea and lemma were removed in I. (J,K) Inner structure of pistils in wild type (J) and *mkb3* (K). The outer integument is not fully elongated in *mkb3*. Arrowheads in J and K indicate the tip of the outer integument. The insets in J and K show higher-magnification views of the tip of the outer integument. The red dotted line in J indicates the outline of the outer integument. n=3 for wild type and n=5 for *mkb3* in B,D,E. Data are mean±s.e.m. and significantly different from wild type where indicated, as assessed by Student's *t*-test (*P<0.05, **P<0.01). Scale bars: 100 µm in J,K.

(ricexpro.dna.affrc.go.jp/). The results showed that *MKB3* was highly expressed in tissues of young inflorescences, moderately in those of pistils, ovaries and early embryos, and at a low level in mature leaf blades and roots. Thus, based on the expression profile of *MKB3* and the phenotype of the *mkb3* mutant, it was predicted that *MKB3* is predominantly expressed in young tissues with active cell proliferation (Fig. 4A), as has been shown for *AN3/AtGIF1* (Horiguchi et al., 2005; Vercruyssen et al., 2014).

Next, we investigated the spatial expression pattern of *MKB3* by *in situ* hybridization. In a longitudinal section of a shoot apex, *MKB3* mRNA was detected mainly in the basal part of young leaf primordia (P1 to P4), and a strong signal was observed in the leaf margins of P2 and P3 primordia. In addition, mRNA was present at the abaxial boundary between a P3 leaf and stem, but not in the SAM (Fig. 4B). In cross-sections, *MKB3* was expressed in the P1, abaxial epidermis and the marginal domain of P2 and P3, but not in the SAM, presumptive vascular bundles or adaxial domain of the inner tissue of P2 and P3 primordia. Expression decreased gradually from the abaxial to the adaxial side of P2 and P3 primordia, although weak expression was detected in the adaxial epidermis of the marginal region (Fig. 4C). In the distal region of the shoot apex, expression was evident in both the adaxial and abaxial epidermis of P2 primordia (a future part of the leaf blade), indicating that the expression pattern differed between the leaf blade and the sheath (Fig. 4D). During reproductive development, a ring-like *MKB3* expression pattern was observed at the nodes of the spikelets and internodes of rachis (Fig. 4E). At the floral organ differentiation stage, *MKB3* expression was mainly detected on the surface of floral organ primordia (Fig. 4F).

These results indicate that *MKB3* is predominantly expressed in the outer layers of younger tissues with high cell proliferation activity. To confirm this, we explored the cell proliferation pattern around the shoot apex using histone *H4* expression as a marker of cell division (Fig. 4G). Histone *H4*-expressing cells were detected in P1, P2 and P3 leaf primordia. Such a cell division pattern was comparable with that associated with *MKB3* expression (Fig. 4C). However, cell proliferation was also observed in regions not expressing *MKB3*, such as the adaxial epidermis of the P3 leaf primordium.

Phenotypic analysis of *MKB3*-overexpressing plants

To further assess the function of *MKB3*, we analyzed *MKB3*-overexpressing plants by introducing a construct harboring *MKB3* cDNA fused to the rice *ACTIN* promoter. Three independent T_1 lines harboring the transgene were obtained (Fig. 5 and Fig. S6), and T_2 plants derived from one of the T_1 line were used (Fig. 5). These plants had normal morphology, but produced longer and wider leaves than control plants, associated with high-level *MKB3* expression (MKB3ox) (Fig. 5A,B,L). The length and width of the fifth leaf blade of MKB3ox plants were 36% and 16%, respectively, greater than those of control plants (Fig. 5D,E). However, cross-sections of MKB3ox and control leaves revealed that the thickness of the fifth leaf blade (Fig. 5C,F), and the size of epidermal cells along the proximal-distal, adaxial-abaxial and medial-lateral axes,

Development (2018) 145, dev159624. doi:10.1242/dev.159624

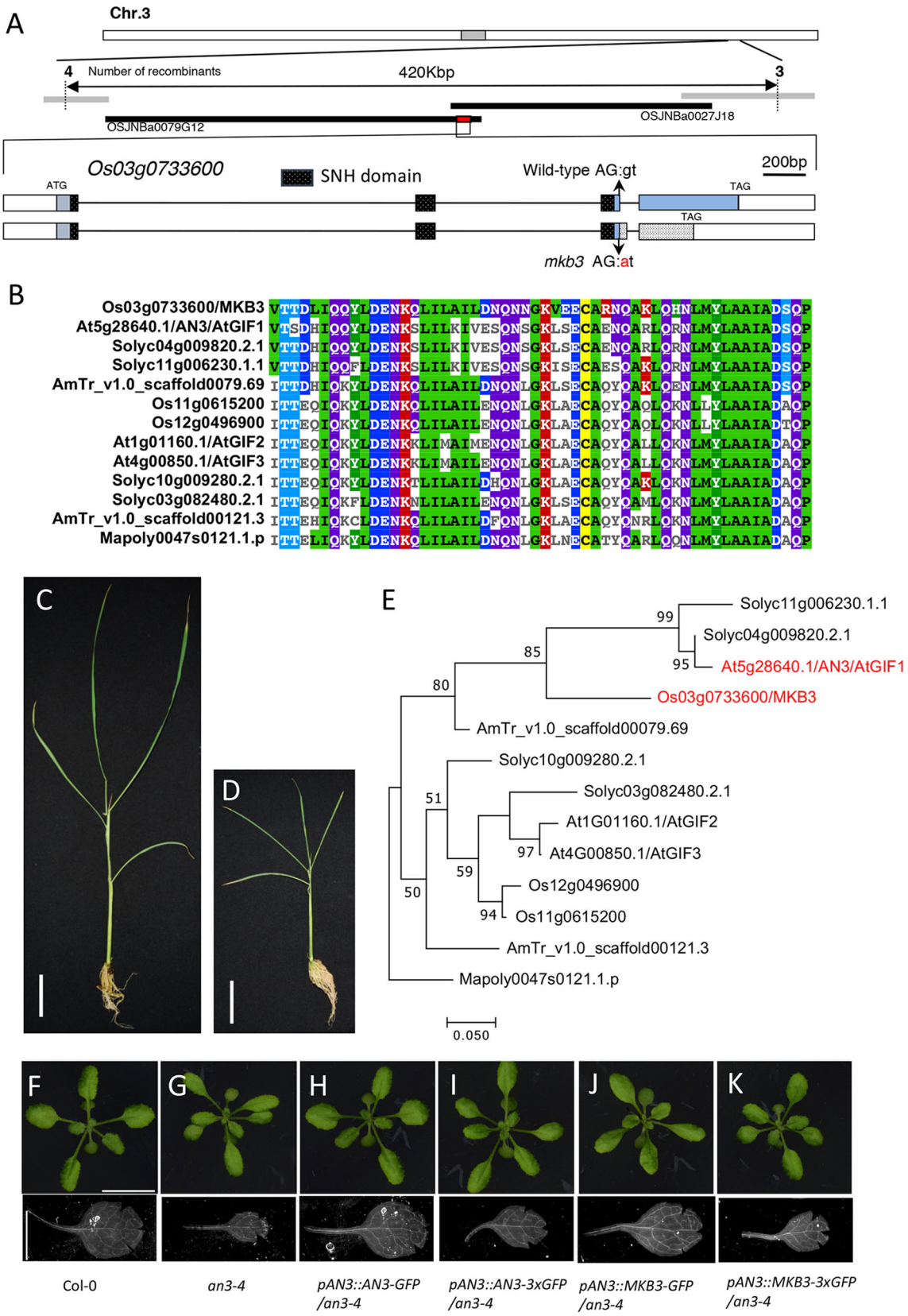

Fig. 3. Cloning of *MKB3*, and the phylogenetic and functional relationships among *MKB3* homologs. (A) Mapping and mutation site of *mkb3*. (B) Multiple alignment of the amino acid sequence of the SNH domain of MKB3 homologs. (C,D) Intraspecific complementation test. (C) *mkb3* plant with a genomic fragment containing MKB3. (D) *mkb3* plant with an empty vector. (E) Phylogenetic tree of *MKB3* homologs. Os, *Oryza sativa*; At, *Arabidopsis thaliana*; AmTr, *Amborella trichopoda*; Solyc, *Solanum lycopersicum*; Mapoly, *Marchantia polymorpha*. (F-K) Interspecific complementation of an *an3-4* mutant by GFP-chimeric proteins with AN3 and MKB3. (F) Wild type, (G) *an3-4*, (H) *pAN3::AN3-GFP*/*an3-4*, (I) *pAN3::AN3-3xGFP*/*an3-4*, (J) *pAN3::MKB3-GFP*/*an3-4* and (K) *pAN3::AN3-3xGFP*/*an3-4* planted 21 days after germination. Lower panels indicate the first leaf. Scale bars: 5 cm in C and D, and 1 cm in the upper and lower panels of F.

Development (2018) 145, dev159624. doi:10.1242/dev.159624

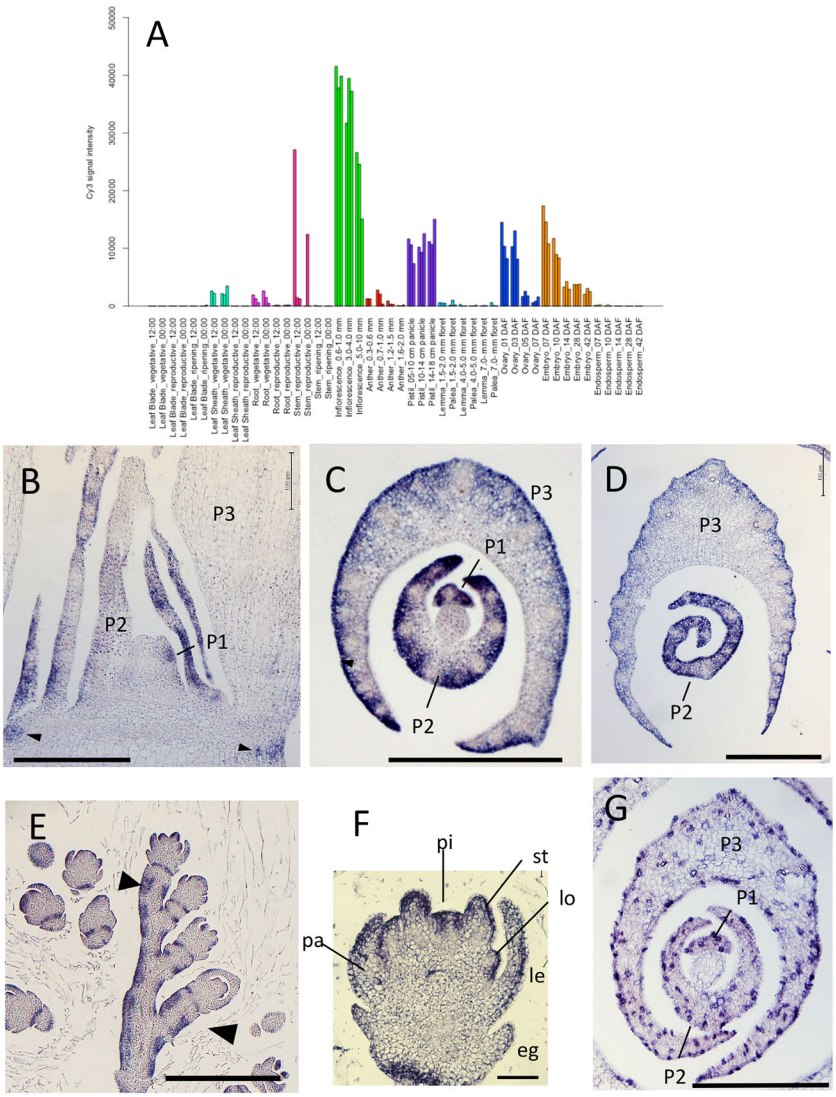

Fig. 4. Expression pattern of *MKB3*. (A) Expression profile of Os03g0733600 (*MKB3*) from the RiceXpro database (ricexpro.dna.affrc.go.jp). (B-E) Spatial expression pattern of *MKB3* by *in situ* hybridization. (B) Longitudinal section of shoot apex 1 month after germination. (C) Cross-section of the basal part of shoot apex 1 month after germination. (D) Cross-section of the P2 leaf blade and P3 leaf sheath 1 month after germination. (E) Longitudinal section of the inflorescence. (F) Longitudinal section of a young flower. (G) Histone *H4* expression pattern in the basal part of the shoot apex 1 month after germination. Plastochron numbers (Px) are labeled in each leaf primordium. Arrowheads in B and E indicate MKB3 expression in the boundary of the nodes. pa, palea; pi, pistil; st, stamen; lo, lodicule; le, lemma; eg, empty glume. Scale bars: 200 µm in B,C,D,G; 500 µm in E; 50 µm in F.

were not significantly different (Table 2). Therefore, it was calculated that the larger leaf size of MKB3ox was due to the increased number of cells, and overexpression of *MKB3* did not affect cell size. In contrast, the number of small vascular bundles and the intervals between the vascular bundles of MKB3ox plants were increased by 17% and 8%, respectively, although the number of large vascular bundles was not altered (Fig. 5A,B; Table 2).

During reproductive development, MKB3ox plants produce longer panicles with longer primary rachis branches compared with control plants, but the number of primary rachis branches was not altered (Fig. 5G-I). MKB3ox plants were fertile and set seeds with significantly larger dimensions along all axes (Fig. 5J,K), as also reported elsewhere (Duan et al., 2015; Li et al., 2016; He et al., 2017). This indicates that overexpression of *MKB3* promotes growth of internodes and seeds, but does not exert harmful effects on tissue differentiation of reproductive organs, in contrast to loss of function of *MKB3*.

Phenotypic analysis of *MKB3*-overexpressing plants suggested that *MKB3* is a positive regulator of cell proliferation. In addition, *MKB3* is not involved in cell size control, because the cell size of MKB3ox plants was not changed. Therefore, cell enlargement in the *mkb3* mutant was a secondary effect of reduced cell proliferation, rather than the direct cause of *MKB3* dysfunction.

Protein movement of MKB3

AN3, the *Arabidopsis* ortholog of *MKB3*, positively regulates cell proliferation in leaves. Although *AN3* mRNA does not accumulate in epidermal cells, *AN3* is required not only by mesophyll cells but also by epidermal cells (Kawade et al., 2013). This is achieved by movement of the AN3 protein from mesophyll cells to epidermal cells. Inter-cell-layer movement of the AN3 protein is essential for coordination of proliferation in mesophyll and epidermal cells, and for regulation of leaf size (Kawade et al., 2013).

MKB3 was strongly expressed in the epidermis of young leaf blades, but weakly or not expressed in the abaxial side of the inner tissues of the P3 leaf sheath, vascular bundles and the SAM (Fig. 4B-D). Thus, the expression patterns of rice *MKB3* and *Arabidopsis AN3* differ markedly.

To determine whether protein movement and its functional importance are conserved between rice and *Arabidopsis*, we performed transgenic analysis using a strategy similar to that of Kawade et al. (2013). We prepared three transgenes: *GFP* as a nonfunctional control, a chimeric gene comprising *MKB3* cDNA fused with *GFP* (*MKB3-GFP*) and *MKB3* cDNA fused with three copies of *GFP* (*MKB3-3×GFP*) as an MKB3 protein mobility control. It is known that the *AN3-3×GFP* protein product is functional but unable to move between cells in *Arabidopsis* leaves

Development (2018) 145, dev159624. doi:10.1242/dev.159624

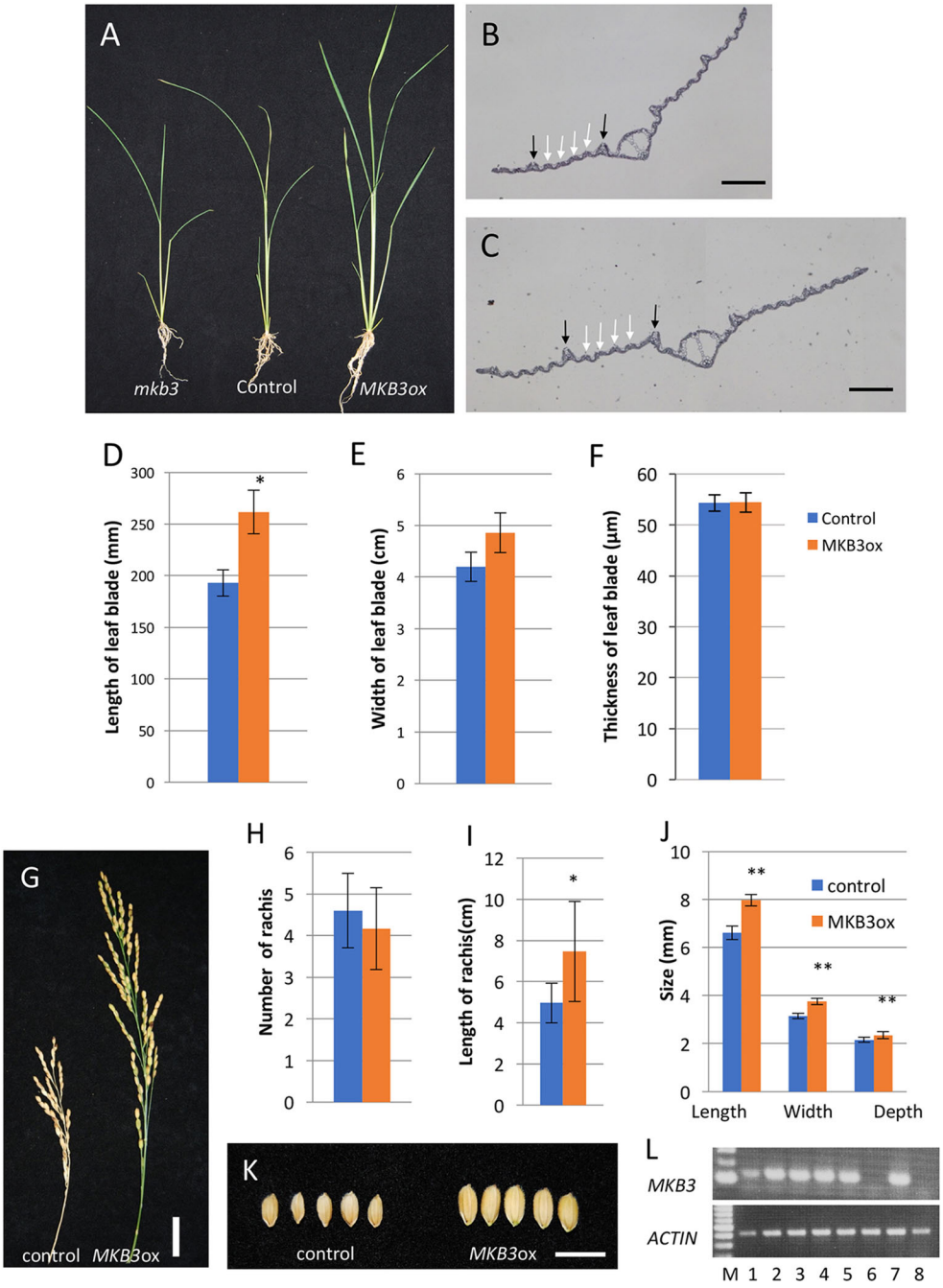

Fig. 5. Phenotypes of *MKB3ox* plants. (A) Seedlings of *mkb3* (left), control (center) and *MKB3ox* (right) 20 days after germination. (B,C) Cross-section of fifth leaf blade in control (B) and *MKB3ox* (C). Black and white arrows indicate the positions of large and small vascular bundles, respectively. (D) Length of the fifth leaf blade. (E) Width of the fifth leaf blade. (F) Thickness of the fifth leaf blade. (G) Wild-type panicle (left) and *mkb3* panicle (right). (H) Number of primary rachis branches. (I) Length of the primary rachis branches. (J) Grain sizes along the three axes. (K) Grains from control (left) and *MKB3ox* (right) plants. (L) Semi-quantitative RT-PCR measuring *MKB3* expression in mature leaves of the T_2 population of *MKB3ox* plants. Upper and lower panels indicate the expression levels of *MKB3* and *ACTIN* (internal control), respectively. M, size marker; 1-8, T_2 plants; 1-5,7 are *MKB3ox* plants. Scale bars: 500 μm in B,C; 3 cm in G; 1 cm in K. *n*=5 in D-F,H-J. Data are mean±s.e.m. and are significantly different from wild type where indicated, as assessed by Student's *t*-test (**P*<0.05, ***P*<0.01).

(Kawade et al., 2010, 2013). These constructs were introduced into wild-type and *mkb3* calli under the control of the native *MKB3* promoter, and five independent T_1 transgenic plants regenerated from wild-type and *mkb3* calli of each line were observed (Fig. 6A).

In the wild-type background, *pMKB3::GFP* (*WT/pMKB3::GFP*) and *WT/pMKB3::MKB3-3×GFP* transgenic plants showed a wild-type phenotype, but *WT/pMKB3::MKB3-GFP* could not be obtained for an unknown reason (Fig. 6B). In the *mkb3* background, *pMKB3::MKB3-GFP* transgenic plants (*mkb3/pMKB3::MKB3-GFP*) showed a phenotype almost identical to the wild-type control, indicating that *pMKB3::MKB3-GFP* is functional and can complement *mkb3* defects (Fig. 6B). However, *mkb3/pMKB3::MKB3-3×GFP* plants produced narrowed and shortened leaves, similar to the *mkb3/pMKB3::GFP* control (Fig. 6B). This suggests that introduction of *pMKB3::MKB3-3×GFP* cannot rescue the *mkb3* phenotype and that MKB3 movement is required for normal leaf development. To explore whether the chimeric MKB3-3×GFP protein was functional, as is true of AN3-3×GFP, we introduced the *AN3-3×GFP* and *MKB3-3×GFP* genes under the control of the *AN3* promoter into *Arabidopsis an3-4* (Fig. 3F,G,I,K and Fig. S5). We found that the extent of phenotypic rescue of *an3-4* leaves by *pAN3::MKB3-3×GFP* was similar to that afforded by *pAN3::AN3-3×GFP*; thus, both *AN3-3×GFP* and *MKB3-3×GFP* mediated partial recovery of leaf size, cell number and cell size (Fig. S5). This strengthened our suggestion that *MKB3-3×GFP* was equivalent to *AN3-3×GFP* in terms of both function and mobility.

Next, we evaluated the protein accumulation pattern in the shoot apex of transgenic plants using GFP to fluorescently detect (Fig. 6C-E) and immunolocalize GFP-tagged proteins (Fig. 6F-H).

Development (2018) 145, dev159624. doi:10.1242/dev.159624

Table 2. Effect of MKB3ox on cell size and the inner structures of leaves

	Control	*MKB3ox*
Length of epidermal cells (μm)*	124.9±19.3	105.9±5.5
Width of epidermal cells (μm)‡	11.7±0.1	10.9±0.8
Thickness of bulliform cells (μm)‡	29.4±0.1	29.2±1.9
Number of large vascular bundles‡	6.0±0	6.4±0.5
Number of small vascular bundles‡	18.0±2.8	21.0±2.2
Interval between vascular bundles (μm)‡	164.7±2.2	178.5±9.8*

*The values were measured using adaxial epidermal cells of the fifth leaf sheath.

‡The values were measured using the fifth leaf blade.

n=25 for cell size, *n*=5 for vascular traits. Figures marked with single asterisks significantly differed from those of the wild type, as assessed using Student's *t*-test to compare epidermal cell sizes and vascular intervals, and the Mann-Whitney test to compare vascular numbers. *P<0.05.

GFP signals in *WT/pMKB3::GFP* and *mkb3/pMKB3::GFP* plants were observed mainly in young leaf primordia, but the tissue specificity was low (Fig. S7), possibly because of GFP protein movement. GFP protein is known to move between cells through plasmodesmata (Kim et al., 2005). GFP signals in *pMKB3::MKB3-3×GFP* plants, which produced an immobile version of MKB3, were predominantly observed in the epidermis and marginal region of leaves, but not in the inner tissue of leaves or the SAM, in both the wild-type and *mkb3* backgrounds (Fig. 6C-E,G). This protein accumulation pattern is generally consistent with that of *MKB3* mRNA determined by *in situ* hybridization (Fig. 4B-D), although MKB3-3×GFP protein accumulation in the epidermis of young leaf primordia and leaf blades was more evident than *MKB3* mRNA (Figs 4C,D, 6F,G). In contrast, the GFP accumulation pattern in *mkb3/pMKB3::MKB3-GFP* was markedly different from that in *WT/pMKB3::MKB3-3×GFP* and *mkb3/pMKB3::MKB3-3×GFP*. GFP signals were detected throughout leaf primordia; i.e. not only in the epidermis but also in the inner tissue, where *MKB3* mRNA was not detected (Fig. 6E,H). In addition, MKB3-GFP protein was detected in the basal part of the SAM, where *MKB3* mRNA was not observed. These results suggest that MKB3-GFP protein moves from an *MKB3*-expressing domain – the epidermis of the leaf – to a non-expressing domain: the inner tissues of the leaf primordia, vascular bundles and the SAM.

DISCUSSION

Phylogenetic analysis indicates that *MKB3* is an ortholog of *Arabidopsis AN3*/*GIF1*. In addition, complementation of *an3* phenotype by *MKB3* indicates that MKB3 protein is functionally equivalent to AN3/GIF1. *AN3*/*GIF1* is not only a central regulator of leaf cell proliferation but also involved in biologically interesting phenomena, such as compensation triggered by mutation of *an3* and inter-cell-layer communication by movement of AN3 (Horiguchi et al., 2005; Kawade et al., 2013, 2017). Thus, *mkb3* could facilitate comparative studies of two evolutionarily diverged species: rice and *Arabidopsis*. Our results indicate that *MKB3* and *AN3* have conserved functions in most aspects, but they are regulated differently in the two species. The similarities and differences between *MKB3* and *AN3* are discussed below.

MKB3 positively regulates leaf size and internode elongation

Although *mkb3* was identified as a mutant with abnormal leaf morphology, our phenotypic analysis revealed that the *mkb3* mutant exhibits abnormalities not only in leaf morphology and size but also in internode and rachis elongation, spikelet and floral morphology, and fertility, indicating that *MKB3* pleiotropically affects plant development during the life cycle in rice. In leaf development, the length and width of the mutant leaf blades were significantly reduced despite the increased size of the cells. This indicates that *MKB3* positively regulates cell proliferation in leaves. This effect of *MKB3* on cell proliferation was supported by the phenotype of *MKB3*-overexpressing plants, which showed increased leaf size with unchanged cell size. In reproductive development, *mkb3* internodes, panicles and rachis were shorter than those of the wild type. Although the cellular responses of these organs and tissues to *mkb3* mutation remain undetermined, the phenotypes possibly suggest that *MKB3* also enhances cell proliferation in stem-like organs during the reproductive phase. This is consistent with the expression of *MKB3* in the basal parts of those organs. In contrast, the number of primary rachis branches was not affected in both *mkb3* mutants and *MKB3*-overexpressing plants. Accordingly, *MKB3* is not involved in branch meristem activity. The reduction of the width of lemma and palea in the *mkb3* spikelets suggests that the growth of these leaf-like organs in the spikelet is under the control of *MKB3*. In addition, the outer integument was incompletely elongated in the *mkb3* pistil, likely also due to a defect in cell proliferation.

Taken together, the role of *MKB3* and *AN3* as positive regulators of cell proliferation in leaves is conserved between rice and *Arabidopsis*. In contrast, abnormalities in stem elongation and floral development were observed in *mkb3* but not in *gif* mutants, suggesting that *MKB3* is required for the development of these organs in rice. However, a *gif1 gif2 gif3* triple mutant of *Arabidopsis* showed reduced stem elongation and abnormal reproductive organ development (Lee et al., 2009). Regarding integument development, a single *an3* mutant showed a shortened outer integument, similar to that in *mkb3* (Lee et al., 2014). Accordingly, although functional redundancy among the paralogs of *Arabidopsis* GIF genes may mask the defects in some plant parts in a *gif1/an3* mutant background, the function of *AN3* and *MKB3* in plant development is largely conserved between rice and *Arabidopsis*. Recently, a *gif1* mutant in maize was reported (Zhang et al., 2018). One of the conspicuous phenotypes was loss of determinacy in axillary meristems, which was observed in neither *Arabidopsis an3* nor rice *mkb3*. Accordingly, the indeterminacy in meristems may be a specific phenomenon of *gif1* mutant in maize.

Compensation occurs both in rice and *Arabidopsis*

Cell size in *mkb3* leaves was increased along the three axes, whereas that in leaves of *MKB3*-overexpressing plants was not changed. This indicated that enlargement of cells in *mkb3* leaves is not a direct effect of *mkb3*, but an indirect effect of decreased cell proliferation or cell number. This is thought to be a typical example of compensation, which is observed in many *Arabidopsis* mutants and transgenic plants, such as *an3*, *fugu1-5*, *erecta*, and *KRP2*-overexpressing plants (Horiguchi and Tsukaya, 2011; Hisanaga et al., 2015). Although compensation in rice was also reported in *OsKRP1*-overexpressing plants (Barrôco et al., 2006), no compensation triggered by a defect in orthologous genes in different species has been reported. In our study, *mkb3*, the counterpart of *Arabidopsis an3*, showed clear compensation, indicating that compensation and its underlying mechanisms are conserved in eudicots and monocots. In addition, the ploidy level in *mkb3* leaves was not altered, although endoreduplication does not normally occur in rice leaves. Thus, cell enlargement in *mkb3* is not caused by ectopic activation of the endoreduplication pathway.

The vascular bundle arrangement in *mkb3* is possibly a compensation-related phenotype. *mkb3* leaf blades have

Development (2018) 145, dev159624. doi:10.1242/dev.159624

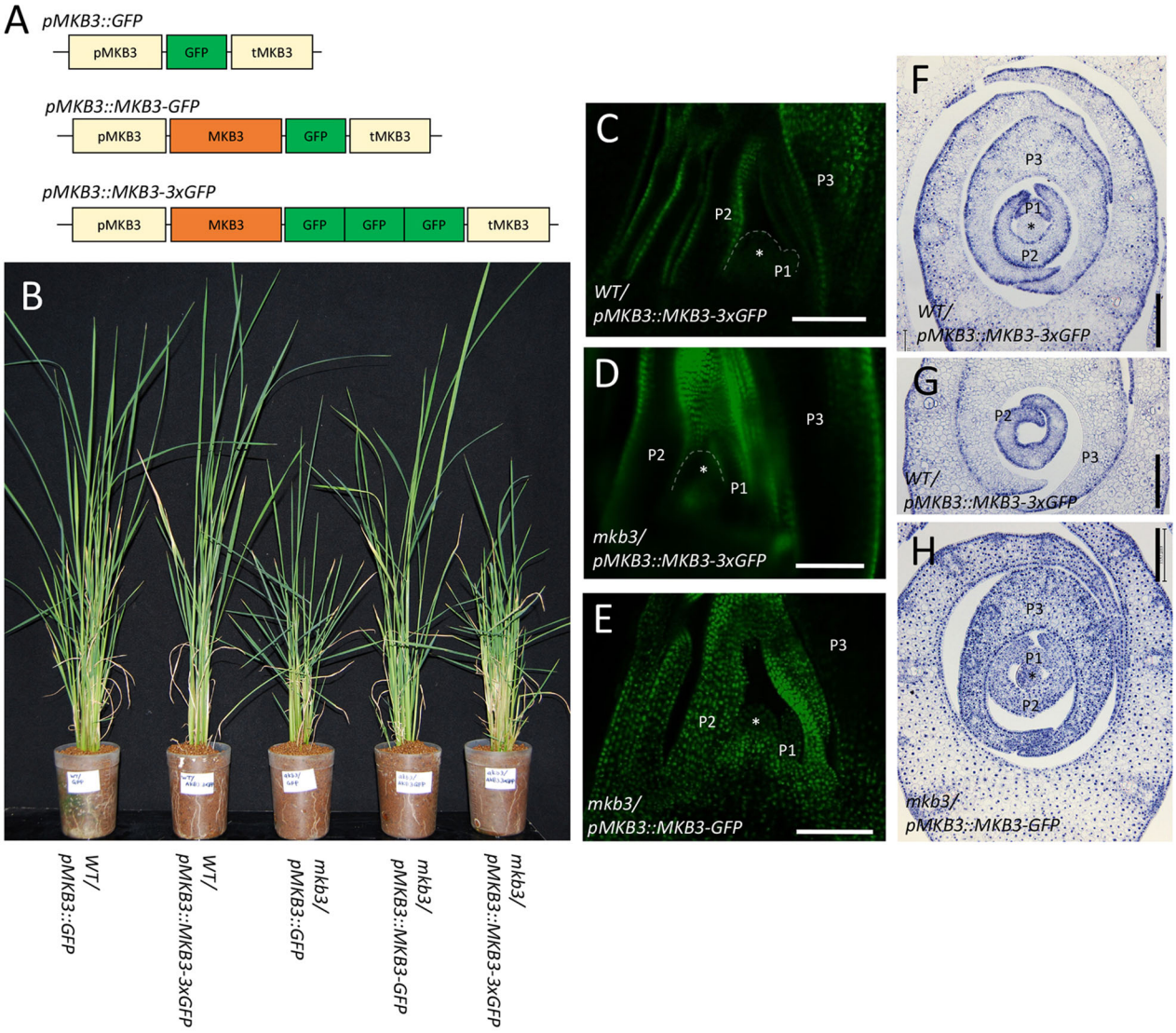

Fig. 6. MKB3 protein movement. (A) Structures of the DNA constructs for GFP and MKB3-GFP fusion proteins. (B) Seedling phenotype of wild type and *mkb3* mutant after introduction of GFP and MKB3-GFP fusion constructs. The *mkb3* mutant plants with *pMKB3::MKB3-GFP* have normal phenotypes. (C-E) Confocal images of GFP fluorescence in shoot apex of transgenic plants. (C) *WT*/*pMKB3::GFP*. (D) *WT*/*pMKB3::MKB3-3xGFP*. (E) *mkb3*/*pMKB3::MKB3-GFP*. (F,G) Immunolocalization of GFP-tagged proteins of transgenic plants 2 weeks after germination. (F) Cross-section of the basal part of *WT*/*pMKB3::MKB3-3×GFP*. (F) Cross-section of the distal part of *WT*/*pMKB3::MKB3-3×GFP*. (G) Cross-section of the basal part of *mkb3*/*pMKB3::MKB3-GFP*. Plastochron numbers (Px) are shown in each leaf primordium. Asterisks indicate shoot apical meristem. Scale bars: 100 µm.

significantly fewer vascular bundles, although the intervals between vascular bundles were slightly increased. The increased intervals of vascular bundles in *mkb3* may be due to the enlargement of cells between vascular bundles by compensation. This explanation is supported by molecular evidence that the position of vascular bundles is determined at the early stage of leaf development before cell expansion starts (Nishimura et al., 2002; Itoh et al., 2005). Thus, compensation affects not only cell and leaf size but also, indirectly, the arrangement of vascular bundles.

MKB3 protein movement

The most conspicuous difference between *MKB3* and *AN3* is their expression patterns. *MKB3* is expressed in younger leaf primordia with active cell proliferation. However, the spatial expression pattern in P2 and P3 primordia is unique in that *MKB3* is predominantly expressed in the epidermal cells of the leaf blade, but not in the mesophyll cells of the adaxial side of the leaf sheath. In contrast, *AN3* mRNA accumulates in mesophyll cells, but not in epidermal cells (Kawade et al., 2013).

In *Arabidopsis*, AN3 protein moves from mesophyll cells to epidermal cells, which facilitates coordination of cell proliferation activity between the different cell layers (Kawade et al., 2013). In rice, MKB3-GFP protein was present not only in epidermal cells but also in inner mesophyll cells where *MKB3* mRNA was not detected, indicating that MKB3 moves from the epidermal cells to the mesophyll cells of leaf primordia. In addition, introduction of immobile MKB3-3×GFP did not rescue the phenotype of *mkb3*. Thus, MKB3 protein movement is essential for a normal cell proliferation pattern in rice leaf, similar to AN3 in *Arabidopsis*.

It is interesting that the direction of movement differs between MKB3 and AN3; i.e. MKB3 moves from epidermal cells to mesophyll cells of leaf blades, and AN3 from mesophyll cells to epidermal cells. In addition, MKB3 moves from the abaxial region to the adaxial regions of leaf sheath primordia. A possible

Development (2018) 145, dev159624. doi:10.1242/dev.159624

explanation for the difference is that the direction of protein movement is associated with the difference in cell proliferation pattern between rice and *Arabidopsis*. During early development of rice leaf, leaf primordia grow in a conical shape to form two structurally different parts: the leaf blades and leaf sheaths (Itoh et al., 2005). Leaf blades are flattened structures, whereas leaf sheaths are crescent-shaped in cross-section. To form a leaf sheath, a decreasing gradient of cell proliferation from the outer (abaxial) region to the inner (adaxial) region of the leaf primordia is essential. Therefore, high cell proliferation activity is more important in the abaxial domain than in the adaxial domain of the leaf sheath. This is also true for organs with a cylindrical or columnar structure, such as internodes and rachis. The *MKB3* expression pattern and MKB3 protein movement may be involved in generating the cell proliferation gradient. That is, MKB3 proteins produced on the abaxial side of the leaf sheath primordia move toward the adaxial side and are diluted, creating a gradient of MKB3 protein amount in the adaxial-abaxial direction. In contrast, coordination in the adaxial-abaxial direction is not necessary in *Arabidopsis* leaves and rice leaf blades, because leaf proliferation activity is similar between the adaxial and abaxial sides of leaf primordia. This notion is supported by the expression pattern of *PLA1*, which is also involved in leaf cell proliferation (Miyoshi et al., 2004; Mimura and Itoh, 2014). Although both rice *PLA1* and its *Arabidopsis* ortholog *KLU* regulate leaf size by controlling cell proliferation, their expression patterns are different. Rice *PLA1* is expressed mainly on the abaxial side of younger leaf sheaths, similar to *MKB3* (Miyoshi et al., 2004). In contrast, *Arabidopsis KLU* does not show a polarized expression pattern in the adaxial-abaxial direction in leaf (Zondlo and Irish, 1999). These polarized expressions of *MKB3* and *PLA1* suggest a requirement for a mechanism of coordinating the cell proliferation gradient during normal leaf development in rice. MKB3 protein movement might be involved in formation of specialized structures such as leaf sheaths, although the complete reversal of the direction of protein movement between the leaf lamina of *Arabidopsis* and the leaf blades of rice remains intriguing.

In summary, rice *MKB3* positively regulates cell proliferation in leaves, and mutant leaves display clear compensation, indicating a conserved function and effect on leaf development of *MKB3* and *Arabidopsis AN3*. In addition, protein movement of MKB3 is essential for normal development of rice leaves. However, the direction of MKB3 movement is different from that of AN3, suggesting that developmental diversity is mediated by expression pattern and/or protein movement, but not by protein function.

MATERIALS AND METHODS

Plant materials and growth conditions

mkb3 was identified as a recessive mutant showing adaxially rolled leaves, and was derived from an M_2 population of rice (*Oryza sativa* L.) cv. Taichung-65 (T-65) mutagenized with N-methyl-N-nitrosourea. Mutant and wild-type plants were grown in pots or in a paddy field. Transgenic plants were grown in a biohazard-secure greenhouse at 30°C during the day and 25°C at night.

Identification of *MKB3*

A heterozygous *MKB3*/*mkb3* plant was crossed with cv. Kasalath (spp. indica), and mutant plants in the F_2 population that exhibited the rolled phenotype were used for mapping. With the aid of cleaved amplified polymorphic sequences and sequence-tagged site markers, the *MKB3* locus was roughly mapped onto the short arm of chromosome 3. Using 224 mutant plants of the F_2 generation, the *MKB3* locus was limited to a region covering two bacterial artificial chromosome (BAC) contigs (OSJNBa0079G12 and OSJNBa0027J18). As we found a homolog of *Arabidopsis AN3* in this region, we compared the nucleotide sequences of the gene between the wild-type and *mkb3* genes.

The *MKB3* cDNA nucleotide sequence and MKB3 amino acid sequence were obtained from GenBank (AK058575 and BR001474). Multiple sequence alignments were performed with the aid of ClustalX. A phylogenetic tree was constructed employing the neighbor-joining method. A *Marchantia polymorpha* sequence served as an outgroup.

Histological analysis

Tissues were fixed in 4% (w/v) paraformaldehyde in 0.1 M sodium phosphate buffer, dehydrated in a graded ethanol series, infused with HistoClear (National Diagnostics) and embedded in Paraplast Plus (McCormick Scientific). Microtome sections (8 µm) were placed on glass slides (Matsunami Glass). For histological observations, sections were stained with Delafield's Hematoxylin and observed under a light microscope. For *in situ* hybridization, digoxigenin-labeled antisense and sense RNA probes for *AKB3* and histone *H4* were prepared. Because the sense probes did not yield specific signals, only antisense probe data are presented here. *In situ* hybridization and immunological detection using alkaline phosphatase were performed using the methods of Kouchi and Hata (Kouchi and Hata, 1993). For immunolocalization of GFP protein, shoot apices of three T_2 transgenic lines: *WT/pMKB3::GFP*, *WT/pMKB3::MKB3-3×GFP* and *mkb3/pMKB3::MKB3-GFP* were sampled 2 weeks after regeneration. The methods were basically those of Smith et al. (1992) with minor modifications. Tissues were fixed, dehydrated and embedded as described above. Dewaxed, rehydrated paraffin sections were treated for 10 min with proteinase K (100 µg/ml in PBS). Slides were incubated in PBS with 1 mg/ml BSA for 30 min, and then with alkaline phosphatase-conjugated anti-GFP antibody (abcam_ab6661) diluted 1:1000 in PBS with 1 mg/ml BSA for 2 h. The remaining steps were identical to those used for *in situ* hybridization.

Measurement of cell size and the traits of vascular bundles

To measure leaf cell sizes in the central-marginal and adaxial-abaxial directions, cross-sections of the fifth leaf blades of wild-type and *pACT::MKB3* plants were prepared. The epidermal cell widths were calculated by dividing the width of the region on the abaxial side of the epidermis in which cells were enumerated by the number of cells. Bulliform cell thickness was measured directly on cross-sections. To measure leaf cell sizes in the distal and proximal directions, the cells of the adaxial surface of the leaf sheath of the fifth leaf were directly observed by fluorescence microscopy. To measure the numbers of vascular bundles and the intervals between them, cross-sections of the fifth leaf blade of wild-type and *pACT::MKB3* plants were evaluated.

Transgenic plants

For intraspecific complementation testing, an 8251 bp genomic fragment of *MKB3*, including the 3308 bp putative promoter and 1898 bp terminator regions was cloned into the pPZP2H-lac binary vector (Fuse et al., 2001). The cloned vector and empty control vector were transformed into *mkb3*-homozygous calli via *Agrobacterium*-mediated transformation (Hiei et al., 1994). For interspecific complementation testing, we used the *pAN3::AN3-GFP* and *pAN3::AN3-3xGFP* transgenic plants described elsewhere (Kawade et al., 2010). *pAN3::MKB3-GFP* and *pAN3::MKB3-3xGFP* transgenic plants were established using binary vectors, R4 pGWB504-*pAN3::OsAN3* and *R4 pGWB501-pAtAN3:OsAN3-3xGFP*, respectively, employing the floral dip method (Clough and Bent, 1998). The vectors were constructed via LR reactions using the Multisite gateway system (Life Technologies) to yield pENTR/D-TOPO-*MKB3* (containing *MKB3* cDNA without a stop codon), pDONR P4-P1R-*pAN3* (containing about 2.0 kb upstream of the *AN3* gene) (Kawade et al., 2013), and binary vectors containing GFP and 3×GFP (Nakagawa et al., 2007). To generate *MKB3*-overexpressing plants, *MKB3* cDNA was inserted into a binary vector containing the rice *ACTIN* promoter and the *NOS* terminator (*pACT::MKB3*) (Kamiya et al., 2003). For phenotypic analysis of *pACT::MKB3*, we used plants harboring *pACT::MKB3* that segregated from the T_2 generation. High-level expression of *MKB3* was confirmed by RT-PCR using RNA samples from leaf tissues of T_2 plants. To evaluate protein movement, *pMKB3::GFP*, *pMKB3::MKB3-GFP* and *pMKB3::MKB3-3×GFP* constructs were prepared. In *pMKB3::GFP*, the

Development (2018) 145, dev159624. doi:10.1242/dev.159624

GFP-encoding sequence was inserted into the *MKB3* fragment within the vector used for complementation testing, and the *MKB3*-encoding sequence was removed. Similarly, a chimeric gene composed of MKB3 cDNA fused with GFP (*MKB3-GFP*) and MKB3 cDNA fused with three copies of GFP (*MKB3-3×GFP*) were introduced between the *MKB3* promoter and the terminator region of the vector. The three constructs were transformed into wild-type and *mkb3* homozygous calli via *Agrobacterium*-mediated transformation (Hiei et al., 1994). All T_1 transgenic plants were evaluated 1 month after regeneration; GFP images around the shoot apices were obtained using a fluorescent microscope (Eclipse-Ti, Nikon) equipped with a confocal laser-scanning system (C1-Si, Nikon). A 488 nm diode laser was used to excite GFP. Emission signals were detected with the aid of a 515/30 nm filter.

Acknowledgements
We thank R. Soga and H. Teshima (Institute for Sustainable Agro-ecosystem Services, The University of Tokyo) for their assistance in cultivating rice plants. We also thank Tomoyuki Takano and Ayaka Kinoshita of the University of Tokyo, who helped with vector constructions.

Competing interests
The authors declare no competing or financial interests.

Author contributions
Investigation: S.S., K.-i.H., T.F., S.-i.A., J.-I.I.; Writing - original draft: J.-I.I.; Writing - review & editing: H.T., J.-I.I.; Visualization: S.A.; Supervision: K.-i.H., H.T., J.-I.I.; Funding acquisition: J.-I.I.

Funding
This work was supported by Japan Society for the Promotion of Science, KAKENHI (16H01230 and 16H04857 to J.-I.I.; 25113002 to H.T.)

Data availability
Sequence data for MKB3 (OsGIF1) (Os03g0733600) complete cDNA and protein can be found in GenBank data libraries under accession number BR001474.

Supplementary information
Supplementary information available online at
http://dev.biologists.org/lookup/doi/10.1242/dev.159624.supplemental

References

Alvarez, P. J., Furumizu, C., Efroni, I., Eshed, E. and Bowman, J. L. (2016). Active suppression of a leaf meristem orchestrates determined leaf growth. *eLIFE* **5**, e15023.

Anastasiou, E., Kenz, S., Gerstung, M., Maclean, D., Timmer, J., Fleck, C. and Lenhard, M. (2007). Control of plant organ size by KLUH/CYP78A5-dependent intercellular signaling. *Dev. Cell* **13**, 843-856.

Barrôco, R. M., Peres, A., Droual, A.-M., De Veylder, L., Nguyen, L. S. L., De Wolf, J., Mironov, V., Peerbolte, R., Beemster, G. T. S., Inze, D. et al. (2006). The cyclin-dependent kinase inhibitor Orysa; KRP1 plays an important role in seed development of rice. *Plant Physiol.* **142**, 1053-1064.

Choi, D., Kim, J. H. and Kende, H. (2004). Whole genome analysis of the OsGRF gene family encoding plant-specific putative transcription activators in rice (Oryza sativa L.). *Plant Cell Physiol.* **45**, 897-904.

Clough, S. J. and Bent, A. F. (1998). Floral dip: a simplified method for *Agrobacterium*-mediated transformation of *Arabidopsis thaliana*. *Plant J.* **16**, 735-743.

Dannenhoffer, J. M., Ebert, W. and Evert, R. F. (1990). Leaf vasculature in barley, *Hordeum vulgare* (Poaceae). *Am. J. Bot.* **77**, 636-652.

Duan, P., Ni, S., Wang, J., Zhang, B., Xu, R., Wang, Y., Chen, H., Zhu, X. and Li, Y. (2015). Regulation of *OsGRF4* by *OsmiR396* controls grain size and yield in rice. *Nat. Plants* **2**, 15203.

Efroni, I., Blum, E., Goldshmidt, A. and Eshed, Y. (2008). A protracted and dynamic maturation schedule underlies Arabidopsis leaf development. *Plant Cell* **20**, 2293-2306.

Ferjani, A., Ishikawa, K., Asaoka, M., Ishida, M., Horiguchi, G., Maeshima, M. and Tsukaya, H. (2013a). Enhanced cell expansion in a KRP2 overexpressor is mediated by increased V-ATPase activity. *Plant Cell Physiol.* **54**, 1989-1998.

Ferjani, A., Ishikawa, K., Asaoka, M., Ishida, M., Horiguchi, G., Maeshima, M. and Tsukaya, H. (2013b). Class III compensation, represented by KRP2 overexpression, depends on V-ATPase activity in proliferative cells. *Plant Signal. Behav.* **8**, e27204.

Fuse, T., Sasaki, T. and Yano, M. (2001). Ti-plasmid vectors useful for functional analysis of rice genes. *Plant Biotech.* **18**, 219-222.

Gonzalez, N., Vanhaeren, H. and Inzé, D. (2012). Leaf size control: complex coordination of cell division and expansion. *Trends Plant Sci.* **17**, 332-340.

He, Z., Zeng, J., Ren, Y., Chen, D., Li, W., Gao, F., Cao, Y., Luo, T., Yuan, G., Wu, X. et al. (2017). OsGIF1 positively regulates the sizes of stems, leaves, and grains in rice. *Front. Plant Sci.* **8**, 1730.

Hervé, C., Dabos, P., Bardet, C., Jauneau, A., Auriac, M. C., Ramboer, A., Lacout, F. and Tremousaygue, D. (2009). In vivo interference with AtTCP20 function induces severe plant growth alterations and deregulates the expression of many genes important for development. *Plant Physiol.* **149**, 1462-1477.

Hibara, K., Isono, M., Mimura, M., Sentoku, N., Kojima, M., Sakakibara, H., Kitomi, Y., Yoshikawa, T., Itoh, J. and Nagato, Y. (2016). Jasmonate regulates juvenile-to-adult phase transition in rice. *Development* **143**, 3407-3416.

Hiei, Y., Ohta, S., Komari, T. and Kumashiro, T. (1994). Efficient transformation of rice (Oryza sativa L.) mediated by Agrobacterium and sequence analysis of the boundaries of the T-DNA. *Plant J.* **6**, 271-282.

Hisanaga, T., Kawade, K. and Tsukaya, H. (2015). Compensation: a key to clarifying the organ-level regulation of lateral organ size in plants. *J. Exp. Bot.* **66**, 1055-1063.

Horiguchi, G. and Tsukaya, H. (2011). Organ size regulation in plants: insights from compensation. *Front. Plant Sci.* **2**, 24.

Horiguchi, G., Kim, G.-T. and Tsukaya, H. (2005). The transcription factor *AtGRF5* and the transcription coactivator AN3 regulate cell proliferation in leaf primordia of Arabidopsis thaliana. *Plant J.* **43**, 68-78.

Ichihashi, Y. and Tsukaya, H. (2015). Behavior of leaf meristems. *Front. Plant Sci.* **6**, 68-78.

Itoh, J.-I., Nonomura, K.-I., Ikeda, K., Yamaki, S., Inukai, Y., Yamagishi, H., Kitano, H. and Nagato, Y. (2005). Rice plant development: from zygote to spikelet. *Plant Cell Physiol.* **46**, 23-47.

Jones-Rhoades, M. W. and Bartel, D. P. (2004). Computational identification of plant microRNAs and their targets, including a stress-induced miRNA. *Mol. Cell* **14**, 787-799.

Kamiya, N., Nagasaki, H., Morikami, A., Sato, Y. and Matsuoka, M. (2003). Isolation and characterization of a rice WUSCHEL-type homeobox gene that is specifically expressed in the central cells of a quiescent center in the root apical meristem. *Plant J.* **35**, 429-441.

Katagiri, Y., Hasegawa, J., Fujikura, U., Matsunaga, S. and Tsukaya, H. and Tsukaya, H. (2016). The coordination of ploidy and cell size differs between cell layers in leaves. *Development* **143**, 1120-1125.

Kawade, K., Horiguchi, G. and Tsukaya, H. (2010). Non-cell-autonomously coordinated organ size regulation in leaf development. *Development* **137**, 4221-4227.

Kawade, K., Horiguchi, G., Usami, T., Hirai, M. Y. and Tsukaya, H. (2013). ANGUSTIFOLIA3 signaling coordinates proliferation between clonally distinct cells in leaves. *Curr. Biol.* **23**, 788-792.

Kawade, K., Tanimoto, H., Horiguchi, G. and Tsukaya, H. (2017). Spatially different tissue-scale diffusivity shapes ANGUSTIFOLIA3 signaling gradient in growing leaves. *Biophys. J.* **113**, 1109-1120.

Kieffer, M., Master, V., Waites, R. and Davies, B. (2011). *TCP14* and *TCP15* affect internode length and leaf shape in Arabidopsis. *Plant J.* **68**, 147-158.

Kim, J. H. and Kende, H. (2004). A transcriptional coactivator, *AtGIF1*, is involved in regulating leaf growth and morphology in Arabidopsis. *Proc. Natl. Acad. Sci. USA* **101**, 13374-13379.

Kim, J. H. and Lee, B. H. (2006). *GROWTH-REGULATING FACTOR4* of Arabidopsis thaliana is required for development of leaves, cotyledons, and shoot apical meristem. *J. Plant Biol.* **49**, 463-468.

Kim, J. H. and Tsukaya, H. (2015). Regulation of plant growth and development by the GROWTH-REGULATING FACTOR and GRF-INTERACTING FACTOR duo. *J. Exp. Bot.* **66**, 6093-6107.

Kim, J. H., Choi, D. and Kende, H. (2003). The AtGRF family of putative transcription factors is involved in leaf and cotyledon growth in Arabidopsis. *Plant J.* **36**, 94-104.

Kim, I., Cho, E., Crawford, K., Hempel, F. D. and Zambryski, P. C. (2005). Cell-to-cell movement of GFP during embryogenesis and early seedling development in Arabidopsis. *Proc. Natl. Acad. Sci. USA* **102**, 2227-2231.

Kouchi, H. and Hata, S. (1993). Isolation and characterization of novel nodulin cDNAs representing genes expressed at early stages of soybean nodule development. *Mol. Gen. Genet.* **238**, 106-119.

Lee, B. H., Ko, J.-H., Lee, S., Lee, Y., Pak, J.-H. and Kim, J. H. (2009). The Arabidopsis *GRF-INTERACTING FACTOR* gene family performs an overlapping function in determining organ size as well as multiple developmental properties. *Plant Physiol.* **151**, 655-668.

Lee, B. H., Wynn, A. N., Franks, R. G., Hwang, Y., Lim, J. and Kim, J. H. (2014). The Arabidopsis thaliana *GRF-INTERACTING FACTOR* gene family plays an essential role in control of male and female reproductive development. *Dev. Biol.* **386**, 12-24.

Li, Y.-F., Zheng, Y., Addo-Quaye, C., Zhang, L., Saini, A., Jagadeeswaran, G., Axtell, M. J., Zhang, W. and Sunkar, R. (2010). Transcriptome-wide identification of microRNA targets in rice. *Plant J.* **62**, 742-759.

Li, S., Gao, F., Xie, K., Zeng, X., Cao, Y., Zeng, J., he, Z., Ren, Y., Li, W., Deng, Q. et al. (2016). The *OsmiR396c-OsGRF4-OsGIF1* regulatory module determines grain size and yield in rice. *Plant Biotechnol. J.* **14**, 2134-2146.
Liu, D., Song, Y., Chen, Z. and Yu, D. (2009). Ectopic expression of *miR396* suppresses GRF target gene expression and alters leaf growth in Arabidopsis. *Physiol. Plant* **136**, 223-236.
Liu, H., Guo, S., Xu, Y., Li, C., Zhang, Z., Zhang, D., Xu, S., Zhang, C. and Chong, K. (2014). *OsmiR396d*-regulated *OsGRFs* function in floral organogenesis in rice through binding to their targets *OsJMJ706* and *OsCR4*. *Plant Physiol.* **165**, 160-174.
Mimura, M. and Itoh, J.-I. (2014). Genetic interaction between rice *PLASTOCHRON* genes and the gibberellin pathway in leaf development. *Rice* **7**, 25.
Miyoshi, K., Ahn, B.-O., Kawakatsu, T., Ito, Y., Itoh, J.-I., Nagato, Y. and Kurata, N. (2004). *PLASTOCHRON1*, a timekeeper of leaf initiation in rice, encodes cytochrome P450. *Proc. Natl. Acad. Sci. USA* **101**, 875-880.
Nakagawa, T., Kurose, T., Hino, T., Tanaka, K., Kawamukai, M., Niwa, Y., Toyooka, K., Matsuoka, K., Jinbo, T. and Kimura, T. (2007). Development of series of gateway binary vectors, pGWBs, for realizing efficient construction of fusion genes for plant transformation. *J. Biosci. Bioeng.* **104**, 34-41.
Nelissen, H., Eeckhout, D., Demuynck, K., Persiau, G., Walton, A., Van Bel, M., Vervoort, M., Candaele, J., De Block, J., Aesaert, S. et al. (2015). Dynamic changes in ANGUSTIFOLIA3 complex composition reveal a growth regulatory mechanism in the maize leaf. *Plant Cell* **27**, 1605-1619.
Nelissen, H., Gonzalez, N. and Inzé, D. (2016). Leaf growth in dicots and monocots: so different yet so alike. *Curr. Opin. Plant Biol.* **33**, 72-76.
Nishimura, A., Ito, M., Kamiya, N., Sato, Y. and Matsuoka, M. (2002). *OsPNH1* regulates leaf development and maintenance of the shoot apical meristem in rice. *Plant J.* **30**, 189-201.
Ori, N., Cohen, A. R., Etzioni, A., Brand, A., Yanai, O., Shleizer, S., Menda, N., Amsellem, Z., Efroni, I., Pekker, I. et al. (2007). Regulation of *LANCEOLATE* by *miR319* is required for compound-leaf development in tomato. *Nat. Genet.* **39**, 787-791.
Rodriguez, R. E., Mecchia, M. A., Debernardi, J. M., Schommer, C., Weigel, D. and Palatnik, J. F. (2010). Control of cell proliferation in Arabidopsis thaliana by microRNA miR396. *Development* **137**, 103-112.
Russell, S. and Evert, R. (1985). Leaf vasculature in *Zea mays* L. *Planta* **164**, 448-458.
Smith, L. G., Greene, B., Veit, B. and Hake, S. (1992). A dominant mutation in the maize homeobox gene, Knotted-1, causes its ectopic expression in leaf cells with altered fates. *Development* **116**, 21-30.
Sun, X., Cahill, J., Van Hautegem, T., Feys, K., Whipple, C., Novák, O., Delbare, S., Versteele, C., Demuynck, K., De Block, J. et al. (2017). Altered expression of maize PLASTOCHRON1 enhances biomass and seed yield by extending cell division duration. *Nat. Commun.* **8**, 14752.
Tsukaya, H. (2002). Interpretation of mutants in leaf morphology: genetic evidence for a compensatory system in leaf morphogenesis that provides a new link between cell and organismal theories. *Int. Rev. Cytol.* **217**, 1-39.
Tsukaya, H. (2014). Comparative leaf development in angiosperms. *Curr. Opin. Plant Biol.* **17**, 103-109.
Tsukaya, H. (2017). Leaf shape diversity with an emphasis on leaf contour variation, developmental background, and adaption. *Semin. Cell Dev. Biol.*, pii: S1084-9521(17)30466-4.
Van Der Knaap, E., Kim, J. H. and Kende, H. (2000). A novel gibberellin-induced gene from rice and its potential regulatory role in stem growth. *Plant Physiol.* **122**, 695-704.
Vercruyssen, L., Verkest, A., Gonzalez, N., Heyndrickx, K. S., Eeckhout, D., Han, S.-K., Jegu, T., Archacki, R., Van Leene, J., Andriankaja, M. et al. (2014). ANGUSTIFOLIA3 binds to SWI/SNF chromatin remodeling complexes to regulate transcription during Arabidopsis leaf development. *Plant Cell* **26**, 210-229.
Wang, L., Gu, X., Xu, D., Wang, W., Wang, H., Zeng, M., Chang, Z., Huang, H. and Cui, X. (2011). miR396-targeted AtGRF transcription factors are required for coordination of cell division and differentiation during leaf development in Arabidopsis. *J. Exp. Bot.* **62**: 761-773.
Wu, L., Zhang, D., Xue, M., Qian, J., He, Y. and Wang, S. (2014). Overexpression of the maize *GRF10*, an endogenous truncated growth-regulating factor protein, leads to reduction in leaf size and plant height. *J. Integr. Plant Biol.* **56**, 1053-1063.
Yang, C. H., Li, D. Y., Mao, D. H., Liu, X., Ji, C. J., Li, X., Zhao, X., Cheng, Z., Chen, C. and Zhu, L. (2013). Overexpression of *microRNA319* impacts leaf morphogenesis and leads to enhanced cold tolerance in rice (Oryza sativa L.). *Plant Cell Environ.* **36**, 2207-2218.
Zhang, D., Sun, W., Singh, R., Zheng, Y., Cao, Z., Li, M., Lunde, C., Hake, S. and Zhang, Z. (2018). *GRF-interacting factor1* (*gif1*) regulates shoot architecture and meristem determinacy in maize. *Plant Cell* **30**, 360-374.
Zhou, M., Li, D., Li, Z., Hu, Q., Yang, C., Zhu, L. and Luo, H. (2013). Constitutive expression of a *miR319* gene alters plant development and enhances salt and drought tolerance in transgenic creeping bentgrass. *Plant Physiol.* **161**, 1375-1391.
Zondlo, S. C. and Irish, V. F. (1999). *CYP78A5* encodes a cytochrome P450 that marks the shoot apical meristem boundary in Arabidopsis. *Plant J.* **19**, 259-268.